Research Square

Preprints are preliminary reports that have not undergone peer review.
They should not be considered conclusive, used to inform clinical practice,
or referenced by the media as validated information.

Adsorption studies of malachite green dye on activated carbon prepared from cocoa biomass

Lourdes Oliveira Galvão
Universidade Federal da Bahia Instituto de Quimica
Gabriel Santos dos Anjos
Universidade Federal do Reconcavo da Bahia
Artur José Santos Mascarenhas
Universidade Federal da Bahia Instituto de Química: Universidade Federal da Bahia Instituto de Quimica
Raildo Alves Fiuza-Junior
Universidade Federal da Bahia, Instituto de Química
Gerônimo Lopes Lima
Universidade Federal do Reconcavo da Bahia
RODRIGO DE PAULA
rodrigodepaula@ufrb.edu.br

Universidade Federal do Reconcavo da Bahia https://orcid.org/0000-0001-8675-3385

Research Article

Keywords: dye, pollutants, malachite green, activated carbon, adsorption kinetics, adsorption thermodynamics

Posted Date: November 25th, 2026

DOI: https://doi.org/10.21203/rs.3.rs-11147494/v1

License: This work is licensed under a Creative Commons Attribution 4.0 International License.
Read Full License

Adsorption studies of malachite green dye on activated carbon prepared from cocoa biomass

Lourdes Oliveira Galvão[a,b,c], Gabriel Santos dos Anjos[a], Artur José Santos Mascarenhas[b,c], Raildo Alves Fiuza-Junior [b,c], Gerônimo Lopes Lima[a], Rodrigo De Paula [a,b,d,*]

[a] Universidade Federal do Recôncavo da Bahia, Centro de Formação de Professores, Av. Nestor de Melo Pita, 535, 45300000, Amargosa/Bahia, Brazil.

[b] Universidade Federal da Bahia, Programa de Pós-Graduação em Energia e Ambiente (PGENAM), Escola Politécnica, R. Prof Aristides Novis, 2, Federação, 40120-910, Salvador/Bahia, Brazil.

[c] Universidade Federal da Bahia, Instituto de Química, Departamento de Química Geral e Inorgânica, Laboratório de Catálise e Materiais (LABCAT), Trav. Barão de Jeremoabo, 147, Campus de Ondina, 40170-280, Salvador/Bahia, Brazil.

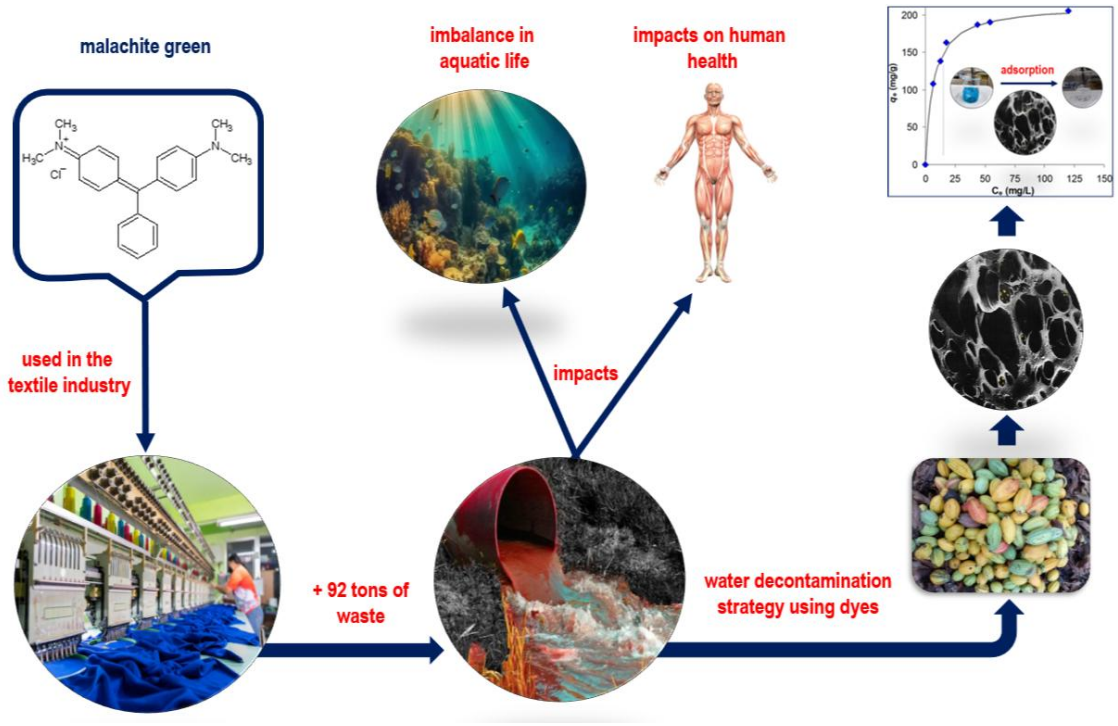
[d] Universidade Federal do Oeste da Bahia, Programa de Pós-Graduação em Química Pura e Aplicada (POSQUIPA), Morada Nobre, 47805-000, Barreiras/Bahia, Brazil.

* Corresponding author:

E-mail: rodrigodepaula@ufrb.edu.br. Phone number: +55 75 991759281

Rodrigo De Paula - ORCID 0000-0001-8675-3385
Artur J. S. Mascarenhas - ORCID 0000-0003-1757-5372
Raildo Alves Fiuza Junior - ORCID 0000-0001-8235-6876
Lourdes Oliveira Galvão – ORCID 0000-0002-8712-3462

Graphical abstract



Highlights

- Residual cocoa biomass as a renewable source for activated carbon preparation;
- Malachite green, a model pollutant contaminant, was removed efficiently in a short time;
- The pseudo-second order kinetic model as well as the Freundlich isotherm describe better the adsorption phenomenon;
- Thermodynamic studies showed spontaneous adsorption up to 65 ºC.

Abstract

The dye malachite green (MG, CI 42000) is widely used in the textile industry to dye various materials and as an antiseptic to treat fish infections. Despite its applications, MG has high toxicity, which causes allergies and skin irritation. This study explored the application of activated carbon prepared from cocoa biomass residue in the removal of organic dyes. Thermogravimetric Analysis, Energy Dispersive X-ray Fluorescence Spectrometry, Fourier Transform Infrared Spectroscopy, Scanning Electron Microscopy, and X-ray Diffraction characterized the biomass and the activated carbon. Adsorption isotherm studies were carried out using the MG dye. Dye removal was monitored spectrophotometrically. The Langmuir and Freundlich models were tested in equilibrium studies, and three kinetic models were evaluated: pseudo first-order, pseudo second-order, and intraparticle diffusion. The kinetic data were best fit to the PSO model, and the adsorption isotherm fit better to the Freundlich model. Those results suggested that chemisorption is the driven force for the process. Thermodynamic data, including a high adsorption enthalpy and a temperature-dependent Gibbs free energy, corroborated such an observation. The results showed that the methodology used to produce activated biochar from cocoa husks (agro-industrial waste) is efficient at removing synthetic dyes.

Keywords: dye, pollutants, malachite green, activated carbon, adsorption kinetics, adsorption thermodynamics.

1. Introduction

The growth of the population and the expansion of industrial activities in sectors such as pharmaceuticals, textiles, leather, plastics, cosmetics, photography, paper and food processing drive the need for new chemically resistant compounds. For such industries, dyes are important substances that give specific color and must be resistant to any adverse situation (wet, sunlight, and so on). During the dyeing process, the residues are discarded improperly. When discarded into water resources without treatment, they cause imbalances in aquatic life, reducing water reoxygenation and hindering sunlight penetration, thereby reducing photosynthetic activity and altering the metabolic processes of aquatic fauna and flora, resulting in microtoxicity for aquatic organisms.

Among the various dyes used in industry, azo dyes are the most widely consumed, playing an essential role in the dyeing of textiles, leather and plastics. Rather than azo compounds, many other dyes are frequently produced for many purposes. Some examples include xanthenes, triphenylmethane, direct, phthalocyanines among other dye classes. However, these dyes and their degradation products are toxic to aquatic life and can cause mutagenic effects in humans. The dyes used in the textile industry are complex organic substances that selectively absorb visible light based on their spectral properties. They appear colored due to the presence of chromophore groups in their molecular structure, such as azo, anthraquinone, polymethine, nitro, nitroso, arylmethane, xanthene, coumarin, and others (Zanoni and Yanamaka 2016). The textile industry contributes significantly to environmental impacts, these industries are responsible for generating more than 92 million tons of waste and are also

classified as some of the largest consumers of water worldwide, consuming an average of 1.5 trillion liters of water per year and contributing approximately 20% to water pollution through their textile treatment and dyeing activities (Sartape et al. 2017).

Malachite Green (MG, CI 42000), a compound belonging to the triphenylmethane dye class, is used in the textile industry to dye cotton, jute, paper, silk, wool, and leather products (Raval et al. 2016; Swan and Zaini 2019). Furthermore, MG is widely used as a topical antiseptic to treat parasites, fungal, and bacterial infections in fish (Pourbabaee et al. 2013; Swan and Zaini 2019). Despite its diverse applications, this dye is highly toxic and can cause problems such as allergies and skin irritations (Dantas et al. 2020).

MG is commonly called aniline green, basic green 4, diamond green B, or victory green B. The nomenclature of MG given by the International Union of Pure and Applied Chemistry (IUPAC) is 4-[(4-dimethylaminophenyl)-phenyl-methyl]-N,N-dimethyl-aniline (Raval et al. 2016). It is a cationic triphenylmethane dye that can be found in chloride or oxalate form (Raval et al. 2016). MG exhibits tautomerism depending on the media. The most common form is the chromatic (Fig. 1-left), but it can also show the carbinol (Fig. 1-centre) and leuko forms (Fig. 1-right). This tautomerism also occurs when ingested and metabolized, where the carbinol form can permeate the cell membrane quickly (Raval et al. 2016).

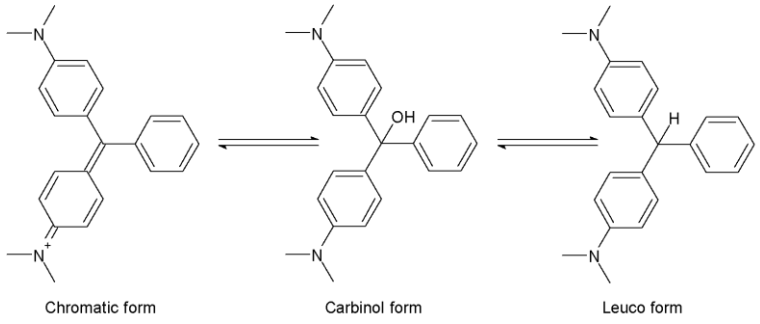


Fig. 1 Chemical structure of malachite green dye and its possible tautomers in solution

Textile industry wastewater poses a significant environmental concern due to its ecotoxicological risks to aquatic life and human health. However, conventional physicochemical treatment methods are often limited in efficiency, as operational parameters such as pH, temperature, and initial dye concentration can compromise the degradation process (Ahmad et al. 2021). Therefore, more effective wastewater decontamination is an important step for the industrial sector in addressing concerns for human health and the environment. The removal of organic dyes from water has been approached through methods classified into three broad groups: chemical, physical, and biological (Xu et al. 2020). The diversity of dyes used in different industrial sectors requires the selection of distinct methods to ensure effective removal. The main physical methods used include adsorption, coagulation/flocculation, and filtration (Zaharia et al. 2024).

The adsorption process has gained notoriety for its cost-effectiveness in removing high-concentration dyes, the absence of unwanted byproducts, and the potential to recover and reuse the adsorbent material. However, for its application in various fields, the adsorption capacity and structure of the adsorbent material are crucial attributes (Zaharia et al. 2024; El Meziane et al. 2025).

In this sense, activated carbon has been a very promising adsorbent material and has been applied in various adsorption processes (El Meziane et al. 2025). Activated carbon can exhibit acidic and basic properties depending on the carbon manufacturing conditions and the oxidation process temperature (El Meziane et al. 2025). The functional groups present on the surface of activated carbon make it a versatile material for materials science, with applications in many fields, particularly in industrial water treatment processes and for medicinal

uses (El Meziane et al. 2025). The use of activated carbons in wastewater treatment is ideal because they can remediate organic pollutants even at low concentrations.

Residual biomass has emerged as a preferred feedstock for activated carbon production due to its cost-effectiveness, and its utilization in synthesizing value-added compounds mitigates improper environmental disposal (Al-Asadi et al. 2025). Aligned with this perspective, the circular economy framework proposes a transition from linear resource flows to closed-loop models. Within this scenario, the objective is to maximize material efficiency to minimize final waste generation (Olofsson and Börjesson 2018; Sherwood 2020).

Table 1 summarizes some residual biomass used to prepare adsorbent materials for adsorption of malachite green dye.

Table 1 Examples of biomass used to remove Malachite Green, procedure of preparation and isothermal model

Entry	Raw material	Process	Removal efficiency, %	Isotherm model	References
1	Rumex abyssinicus	Activation with H_3PO_4 at a 1:1 ratio (w/v); Pyrolysis in a furnace at 500 °C for 2 h	99.9% – 62.4% dye removal	Single-layer chemisorption; Koble–Corrigan isotherm model.	(Abewaa et al. 2023)
2	Cashew fruit mesocarp (Anacardium occidentale)	Activation with NaOH; Pyrolysis in a muffle furnace at 400 °C (1h)	99.6% – 79.07% dye removal	Monolayer chemisorption; Langmuir isotherm model	(Da Silva et al. 2021)
3	Açaí seed (Euterpe oleracea)	Acid activation (H_3PO_4) and basic activation (NaOH); Carbonization at 400 °C (1h)	CAG-A: 91.5% – 78.5% dye removal CAG-B:	Multilayer chemisorption; Freundlich isotherm model	(De Sousa et al. 2021)

4	Banana peel and corn cob (*Musa* spp. And *Zea mays* L.)	Washed and ground; Acid activation (HCl) and basic activation (NaOH)	98% – 96.8% dye removal Banana (AB): 99.09% dye removal Corn (AA): 90.85% dye removal	Freundlich isotherm model	(Dantas et al. 2020)
5	Silk flower (Calotropis procera)	*In natura* Fibers and treated with NaOH (0.1 M e 1 M)	CPST: 51.14% CPCT 0.1M: 36.75% CPCT 1M: 48.86%	Elovich and Intraparticule diffusion model	(Oliveira 2024b)
6	Green coconut (Cocos nucifera)	*In natura* material; Washed, ground and dried	91.95% – 85.5% dye removal	Monolayer chemisorption; Temkin isotherm model	(Silva AAD 2021)
7	Pineapple crown (Ananas comosus)	Ground, washed and pyrolysis at 600 °C (3h)	80% dye removal	Chemisorption; Sips isotherm model	(Santos 2020)
8	Fe_3O_4/MgAl-LDH (Composite)	Coprecipitation of Mg^{2+}, Al^{3+} and Fe_3O_4 in NaOH	Composite: 100% MgAl-LDH: 100% Fe_3O_4: 80%	Monolayer chemisorption; Sips isotherm model	(Sá 2021)
9	Sawdust powder (Pinus sp.)	*In natura* material; oven-dried at 105 °C (24h)	94.6% dye removal	Chemisorption; Freundlich isotherm model	(Silva LF 2014)
10	Carnauba (Copernicia prunifera)	Washed, Ground and dried at 60 °C	96% dye removal	Chemisorption; Langmuir isotherm model	(Oliveira 2024a)

The concept of a circular bioeconomy is an emerging paradigm widely debated across academic, political, and industrial spheres, integrating the

principles of the circular economy, bioeconomy, and green economy. The bioeconomy is defined as the utilization of renewable biological resources for generating novel materials, value-added products, and energy. Concurrently, the green economy serves as an overarching framework that integrates circular economy and bioeconomy principles alongside contemporary approaches, such as nature-based solutions. Conversely, the circular bioeconomy specifically aims to promote the sustainable utilization of biomass, incentivizing waste reuse and valorization within a sustainable, closed-loop consumer perspective (Olofsson and Börjesson 2018; Sherwood 2020).

Biomass plays a pivotal role in the circular economy by facilitating the conversion of organic waste into raw materials for energy generation, biofuel production, and the synthesis of advanced materials. As demonstrated by James Sherwood (2020), the circular economy relies on maximizing resource efficiency and minimizing waste generation, rendering biomass a strategic asset due to its inherent renewability through natural biological cycles. Furthermore, the sustainable exploitation of agricultural, forestry, and food waste contributes to mitigating reliance on fossil resources, reducing greenhouse gas emissions, and fostering sustainable production systems. The study further emphasizes that biomass valorization within a circular bioeconomy requires systemic integration among production, consumption, and waste management, thereby enhancing material and energy recovery throughout the entire value chain (Sherwood 2020).

Global cocoa production continues to solidify its position as a critical agricultural commodity in the international market. According to data from the Brazilian Institute of Geography and Statistics (IBGE 2025) and the Technical Office for Economic Studies of the Northeast (ETENE), Côte d'Ivoire and Ghana

are the leading global cocoa producers, collectively accounting for approximately half of world production. Within the Americas, Ecuador is the largest producer, commanding 9.6% of the global output in the 2023/24 crop year, followed by Brazil at 4.5%, with the states of Pará and Bahia driving domestic production. For the 2023/24 crop year, global cocoa bean production was estimated at 4.8 million metric tons.

However, this substantial production highlights a critical sustainability bottleneck: the chocolate industry utilizes only about 30% of the total fruit biomass (the beans), resulting in a stark disparity where approximately 10 tons of waste are generated for every ton of processed cocoa (Anoraga et al. 2024; Sotelo-Coronado et al. 2025). This surplus biomass, primarily comprising the cocoa pod husk, pulp, and teguments, amounts to tens of millions of tons annually and is frequently discarded in landfills or abandoned on plantations. Such practices not only neglect the economic potential of these bioactive-rich byproducts but also exacerbate environmental degradation through greenhouse gas emissions and the proliferation of phytopathogens. Consequently, residual management has become one of the most pressing challenges within the contemporary agricultural bioeconomy (Anoraga et al. 2024; Sotelo-Coronado et al. 2025).

Within this framework, the circular economy and bioeconomy offer strategic alternatives to convert cocoa waste into value-added feedstocks, thereby enhancing resource efficiency and mitigating the environmental impacts associated with improper disposal (Ferrão-Gonzales et al. 2013). In Brazil, particularly in prominent producing regions like southern Bahia, research has demonstrated the potential of residual cocoa biomass for applications in

bioenergy, organic fertilizers, biochar, biopackaging, biopolymers, and adsorbent materials (Ferrão-Gonzales et al. 2013; Girón-Hernández et al. 2024).

Beyond minimizing waste generation and greenhouse gas emissions, valorizing these byproducts fosters economic diversification within the cocoa value chain, upgrades agro-industrial waste, and reinforces sustainable production systems. Thus, the comprehensive valorization of cocoa biomass aligns with circular bioeconomy principles, transforming an environmental liability into a strategic resource for technological innovation and sustainable development (Ferrão-Gonzales et al. 2013; Girón-Hernández et al. 2024; Sotelo-Coronado et al. 2025).

This study aims to evaluate the adsorption capacity of activated carbon synthesized from cocoa shells—the primary biomass residue in the cocoa value chain—for the removal of Malachite Green dye, selected as a model contaminant, from aqueous solutions.

2. Materials and methods

2.1. Biomass collection and characterization

The cocoa shell biomass used in this study was collected in the rural area of the city of Amargosa/BA-Brazil (13° 01′ 48″ S, 39° 36′ 18″ W). After collecting, the cocoa shells were weighed and cut into small pieces measuring approximately 2 cm x 2 cm. They were oven-dried for 24 h at 110 °C. After drying, the shells were ground in a knife mill and sieved through a set of sieves with an 80-100 mesh screen. The biomass was characterized by Thermogravimetry (TG/DTA), according to ASTM E1757 and E1755 standards, to determine humidity, volatile carbon, fixed carbon, and ash content, as well as to estimate

biomass macrocomponent composition. X-ray Fluorescence performed elemental analysis. Powder X-ray Diffractometry investigated biomass crystallinity.

2.2. Adsorbent preparation

The activated carbon was prepared from cocoa biomass by pyrolysis. Cocoa shell biomass was treated in a vertical reactor (with Φ = 5.0 cm) coupled to a tubular furnace. Pyrolysis was carried out under an inert atmosphere (N_2) at a flow rate of 150 mL min^{-1}. The temperature was raised at a heating rate of 5 °C min^{-1} to 800 °C, then held for 2 hours. At the end of the reaction time, the resulting carbon was removed from the reactor, washed with 1 mol L^{-1} hydrochloric acid, and finally separated by vacuum filtration (Figure 2).

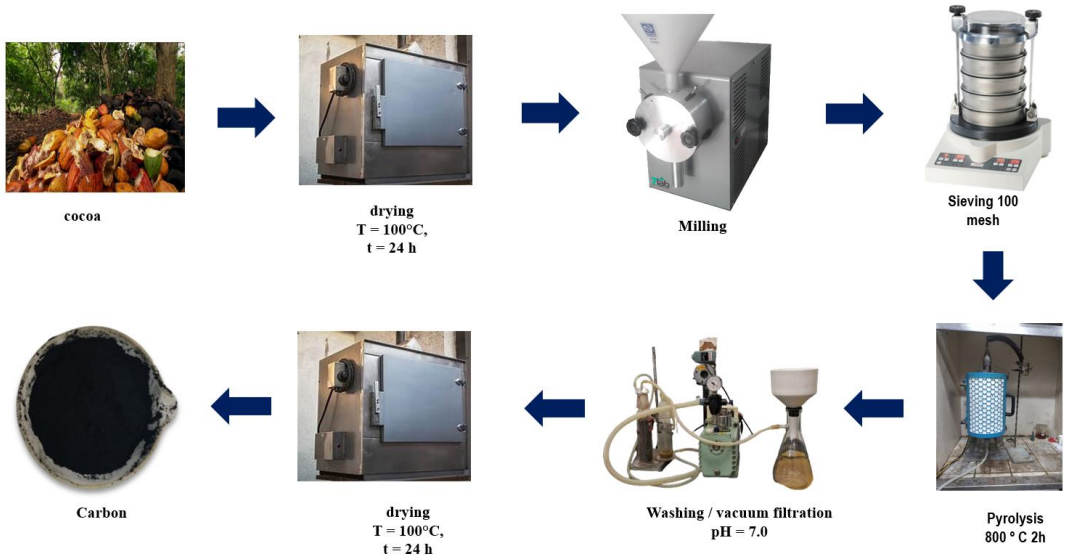


Fig. 2 Activated carbon preparation from cocoa residual biomass

2.3. Characterization of biomass waste and activated carbons

Elemental analysis was performed by Energy Dispersive X-ray Fluorescence Spectrometry (EDX) on a Shimadzu spectrometer, model EDX-720, with a rhodium radiation source operating at 15 kV (Na to Sc) and 50 kV (Ti to U), and a 10 nm collimating slit. The samples were analyzed as powders in a 5nm diameter polypropylene cell. Thermogravimetric analyses were performed on a Shimadzu DTG-60H instrument under a N_2 atmosphere at a flow rate of 50 mL min^{-1} and a heating rate of 10 °C min^{-1} (25 – 900 °C), using ~15 mg of material. FTIR analyses were performed on a Perkin-Elmer Spectrum 400 FT-IR-NIR Spectrometer with a Fourier transform infrared spectrometer. Spectra were obtained in the region from 4000 to 400 cm^{-1} using 0.1% KBr wafers with a resolution of 4 cm^{-1}. X-ray diffraction patterns using a Shimadzu XRD-6000 diffractometer, operating with monochromatic CuKa radiation at 40 kV and 30 mA. The morphology of the materials was investigated by scanning electron microscopy (SEM) using a Hitachi S-3400N microscope, with samples dispersed on carbon tape and without prior metallization.

2.4. Determination of Point of Zero Charge

To determine the point of zero charge (PCZ), 20 mL of solution with initial pH (pH_i) concentrations ranging from 1 to 13 (1, 3, 5, 7, 9, 11, and 13) was initially distributed among seven beakers. The pHi was adjusted with 1.0 mol L−1 HCl and NaOH solutions using a Tecnopon model mPA-210 MS pH meter. After that, 10 mg of the activated carbon from cocoa shell biomass was added to each

beaker. The solutions were stirred continuously (1,500 rpm) for 24 h in a closed system at room temperature on an IKA magnetic stirrer, model C-MAG HS 7. After filtering the samples, the final pH (pH_f) of the filtrate was measured. The graph of pH variation (ΔpH = pHi−pHf) versus pHi provided the PCZ at the intersection point (ΔpH = 0).

2.5. Adsorption studies

2.5.1. Adsorption isotherms

Adsorption isotherm studies with activated carbon were performed at 30 °C and 800 rpm stirring for 4h using four different concentrations. The dye used in the adsorption experiments was the chloride form of malachite green (MG, $C_{23}H_{25}ClN_2$) with a molar mass of 364.90 g mol^{-1}. Malachite green dye solutions at different concentrations were prepared from a stock solution at 364.9 mg L^{-1}. The studies were performed by adding 100 mg of activated carbon to a definite volume of each of these solutions. The amount of dye adsorbed in equilibrium with the dye in solution was obtained by equation 1.

$$q = \frac{(C_0 - C_e).V}{m} \quad (1)$$

where: *q* = adsorption capacity (mg g^{-1}); *Co* = initial adsorbate concentration (mg L^{-1}); *Ce* = adsorbate concentration at equilibrium (mg L^{-1}); *V* = volume of solution (L); *m* = mass of adsorbent (g).

Two adsorption isotherm models, Langmuir and Freundlich, were applied to the experimental data set. The Langmuir isotherm is a theoretical model used to describe the adsorption of solutes from a liquid solution onto a surface. Langmuir assumes that adsorption occurs in a monolayer, in which the adsorbent

has a finite number of identical adsorption sites. This model assumes that adsorption energies are uniform across the surface and that adsorbed molecules do not move along the surface (Sartape et al. 2017; Nascimento et al. 2020). Therefore, the Langmuir isotherm is often used to estimate the maximum adsorption capacity, which corresponds to the complete coverage of the adsorbent surface by a single layer of molecules. The Langmuir equation (Eq. 2) is commonly expressed in the following form, according to Nascimento et al. (2020):

$$q = \frac{q_{max} K_L C_e}{1 + K_L C_e} \quad (2)$$

where: q = amount of solute adsorbed per gram of adsorbent at equilibrium (mg g^{-1}); q_{max} = maximum adsorption capacity (mg g^{-1}); K_L = adsorbate/adsorbent interaction constant (L mg^{-1}); Ce = adsorbate concentration at equilibrium (mg L^{-1}).

To determine the values of q_{max} and K_L, the Langmuir equation is usually linearized. Thus, by plotting Ce/qe as a function of Ce, the values of q_{max} and K_L can be obtained from the coefficients of the linear equation.

The Freundlich model was one of the first to establish a mathematical relationship for adsorption, connecting the amount of adsorbed material to its concentration in solution. As an empirical model, it stands out for its applicability to non-ideal systems, such as those with heterogeneous surfaces and multilayer adsorption. The model accounts for surface heterogeneity by applying an exponential distribution to characterize sites with different adsorption energies (Sartape et al. 2017; Nascimento et al. 2020). The Freundlich equation (Eq. 3) is commonly expressed in the following form, according to Nascimento et al. (2020):

$$q = K_F C_e^{1/n} \quad (3)$$

where: *q* = amount of adsorption at equilibrium (mg g^{-1}); *Ce* = concentration of adsorbate at equilibrium (mg L^{-1}); *1/n* = constant related to surface heterogeneity; K_F = Freundlich adsorption capacity constant (mg g^{-1} (mg $L^{-1})^{1/n}$).

Thus, for determining the K_F and 1/n parameters from linear regression, a plot of q versus log Ce will provide a slope of 1/n and an intercept of log K_F (Nascimento et al. 2020)

2.5.2. Adsorption kinetics

Adsorption kinetics studies with MG dye on activated carbon were performed for three systems (C1 = 75 mg L^{-1}; C2 = 100 mg L^{-1}; and C3 = 150 mg L^{-1}) at three different temperatures (30 ºC, 40 ºC, and 50 ºC) and with stirring at 800 rpm for 20 min. The monitoring of the dye removal from the solution was performed by reading in a spectrophotometer at the wavelengths of its maximum absorption wavelengths, 421 nm and 615 nm. Spectrophotometer Global Trade Technology; model: UV-5100 was used where the scans were performed at 1, 3, 5, 7, 10, 15, and 20 minutes.

To describe adsorption kinetics, three mathematical models were tested: pseudo-first-order, pseudo-second-order, and intra-particle diffusion. All fits were performed using linearized equations.

The PFO kinetic model (Eq. 4), also known as the Lagergren model, is commonly used to predict CO_2 physisorption on physical adsorbents. In this model, the adsorption rate is directly proportional to the number of available adsorption sites on the adsorbent (Enayatpour et al. 2018). The linear form of the pseudo-first order rate equation is expressed as follows:

$$ln(q_e - q_t) = lnq_e - k_1 t \quad (4)$$

The PSO kinetic model (Eq. 5) is ideal for predicting CO_2 chemisorption on adsorbents. This model assumes a linear relationship between the CO_2 adsorption rate and the square of the number of unoccupied adsorption sites (Largitte and Pasquier 2016). The linear form of the pseudo-second order rate equation is expressed as follows:

$$\frac{t}{q_t} = \frac{1}{k_2.q_e^2} + \frac{t}{q_e} \quad (5)$$

Where: q_e (mmol g^{-1}) and q_t (mmol g^{-1}) represent, respectively, the equilibrium CO_2 adsorption capacity and the amount of CO_2 adsorbed at time t (s). k_1 denotes the first-order kinetic constant, and k_2 denotes the second-order kinetic constant.

The Weber and Morris intraparticle diffusion model (Eq. 6) is based on molecular transfer within the pores of the solid (Zhang et al. 2018). The equation describing the relationships between the parameters for intraparticle diffusion is:

$$q_t = K_{id} t^{1/2} + C \quad (6)$$

where C is the intercept and k_{id} (mg/g $min^{1/2}$) is the intraparticle diffusion rate constant, which can be calculated from the slope of the linear plot of q_t versus $t^{1/2}$.

2.5.3. Effect of temperature and thermodynamic parameters

The temperature-dependent experiments were conducted to estimate the thermodynamic parameters of the adsorption process. For that, the equilibrium constant was calculated according to Equation 7, and the enthalpy and entropy of the adsorption process were calculated using equation 8.

$$K_{eq} = \frac{q_e}{C_e} \quad (7)$$

$$ln\, K_{eq} = \frac{\Delta_{ads}S}{R} - \frac{\Delta_{ads}H}{R}.\frac{1}{T} \quad (8)$$

where: R = universal gas constant (8.314 J mol^{-1} K^{-1}), T = temperature (K), and K_{eq} is the thermodynamic equilibrium constant.

3. Results and discussion

3.1. Biomass characterization

The results of the immediate analysis of cocoa biomass, applying ASTM standards, were 11.2% moisture, 6.7% ash, 79.6% volatiles, and 2.3% fixed carbon. Similar results were reported in the literature in relation to cocoa shell biomass, which presented moisture contents ranging from 8 to 12%, ash contents between 5 and 8%, volatile matter around 70 to 80% and fixed carbon normally below 20% before carbonization (Pereira et al. 2014).

Elemental analysis by EDX (Table 2) of the ash revealed higher concentrations of the elements potassium (K) and calcium (Ca). The high concentration of potassium is enough to provide activated carbon, since potassium can act as an activator during the pyrolysis process. Also, considering the macronutrients fertilizers (N, P, K), this activated carbon can be considered for soil nutrition in agricultural management. Beyond its mineral value, cocoa biomass stands out as a source of natural resources rich in phytochemicals, such as polyphenols, enzymes, and sugars (Anoraga et al. 2024; Sotelo-Coronado et al. 2025). The preparation of these bioactive compounds opens up opportunities for use in high-value-added sectors, including the cosmetics, pharmaceutical, and flavor industries (Anoraga et al. 2024; Sotelo-Coronado et al. 2025). Therefore, improving integrated management of these residues in the cocoa

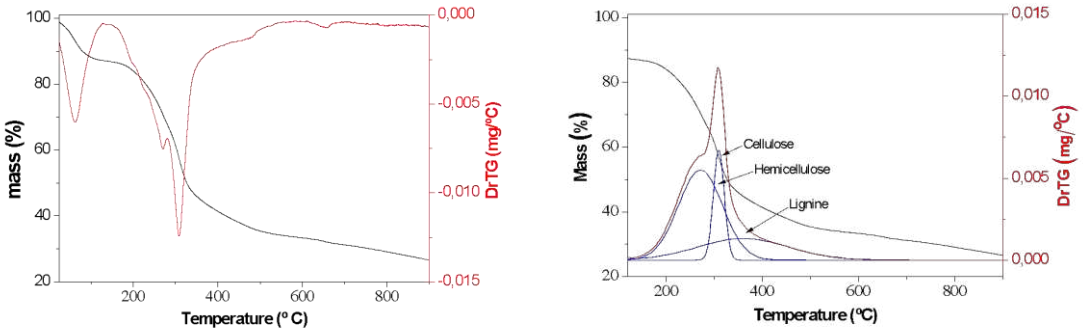
industry not only mitigates food waste but also promotes sustainability and the generation of economic value from byproducts.

Table 2 Elemental composition of biomass ash obtained by EDX

Element	**K**	**Ca**	**Mg**	**Fe**	**S**	**P**	**Zn**
Content, %	79.53	14.34	0.99	2.17	0.88	0.63	0.36
Standard deviation	± 1.02	± 0.16	± 1.05	± 0.13	± 0.02	± 0.01	± 0.04
Element	**Rb**	**Mn**	**Cr**	**Si**	**Cu**	**Sr**	**-**
Content, %	0.30	0.25	0.08	0.23	0.12	0.13	-
Standard deviation	± 0.01	± 0.017	± 0.13	± 0.06	± 0.01	± 0.003	-

The analysis of the thermal decomposition of biomass residues presented thermogravimetric curves (Figure 3a), with four regions of mass loss: i) The mass loss between 60 ºC and 100 °C is related to the loss of biomass moisture, in which, as the temperature increases, the water present in the sample evaporates. The water present in biomass occurs in two forms: free water and "bound" water. Free water evaporates more rapidly up to 100 °C due to its weak interaction with the biomass, while bound water has a stronger interaction with the biomass and can evaporate at temperatures up to approximately 150 °C (Fiuza-Junior 2016); ii) mass losses in the range between 160 ºC and 400 °C are associated with the thermal decomposition of hemicellulose; iii) the third region of mass loss at approximately 270 ºC to 400°C is related to cellulose degradation; and iv) a fourth phenomenon occurs in a wide range of approximately 160 ºC to 600 °C, corresponding to the thermal degradation of lignin (Fiuza-Junior 2016).

The DTG curve in Figure 3b was deconvoluted to quantify the biomass components using Gaussian curves, with a correlation coefficient (R^2) of 0.9983.



(a) (b)

Fig. 3 Thermogravimetric analysis of **(a)** cocoa biomass and **(b)** DTG deconvolution. Conditions: mass = 15 mg, heating rate = 10ºC min^{-1}, nitrogen flow = 50 mL min^{-1}

Table 3 presents the estimated composition of lignocellulosic components by volatilization, obtained by the Gaussian area of the macrocomponents. Hemicellulose accounted for 44.7%, followed by cellulose at 13.5% and total lignin at 22.0%. Lignin content is an important factor, as it influences the formation of fixed carbon. The observed content is similar to that typically found in biomass used for activated carbon production, ranging from 13% to 40% (Rout et al. 2016; Neme et al. 2022).

Table 3 Estimated composition for cocoa biomass

Macrocomponent	Peak region (°C)	%
Hemicellulose	160 - 400	44.7
Cellulose	270 - 400	13.5
Lignin	160 - 600	22.0

3.2. Adsorbent characterization

The powder X-ray diffraction patterns of the biomass residue and the activated carbon sample are shown in Figure 4. The samples consist mainly of

an amorphous carbon matrix. The samples consist mainly of an amorphous carbon matrix. In the case of biomass, the behavior observed in the XRD refers to the crystalline domains of cellulose, which form a narrower halo, while the rest of the signal refers to amorphous cellulose. For activated carbon, two halos characteristic of amorphous materials are observed at approximately 2θ = 29.28º and 43.10º. These halos indicate a small amount of crystalline material that may be related to the graphitic structure (Suresh et al. 2011; Cai et al. 2014; Fiuza-Junior et al. 2016).

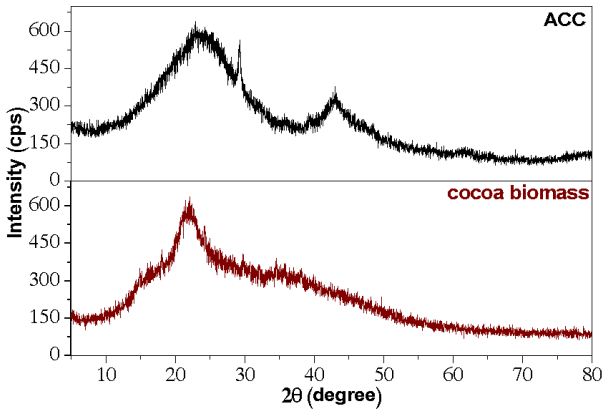
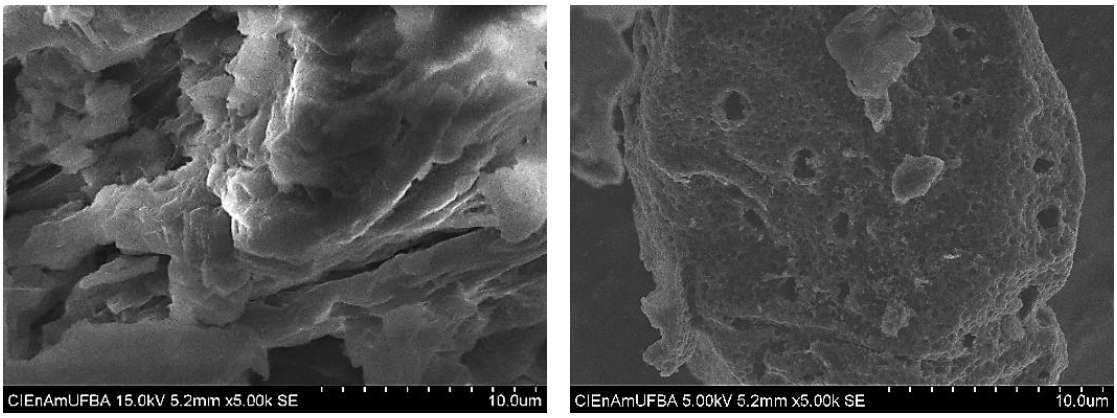


Fig. 4 X-ray diffraction of cocoa biomass and activated carbon

Scanning electron microscopy was used to observe the morphology of the biomass residue and activated carbon (Figure 5). The micrographs reveal that the biomass (Figure 5a) has irregular, rough surfaces, characteristic of lignocellulosic compounds (Alfa et al. 2024). After biomass pyrolysis at 800 °C (Fig. 5b), a morphological change is observed on the charcoal surface, with the formation of pores and an increase in roughness compared to the raw biomass micrograph (Fig. 5a).



(a) (b)

Fig. 5 Scanning electron microscopy (SEM) of **(a)** cocoa biomass residues and **(b)** activated carbon

Adsorbent surface studies are extremely important for understanding the adsorption process. The potential of zero charge (pHPZC) indicates the pH at which the net charge on the adsorbent surface is zero (Essandoh et al. 2016). According to the method used to determine the point of zero charge, the pH_{PZC} value is the point at which the ΔpH (pH_f-pH_i) versus pHi curve crosses the zero line. The pH_{PZC} of the activated carbon under study is approximately 6.8 (Figure 6). This study is important because, in adsorption processes, the adsorbate and adsorbent charges should be opposite to allow stronger electrostatic interactions. When the charges are equal, adsorption may be impaired by electrostatic repulsion (Nascimento et al. 2020).

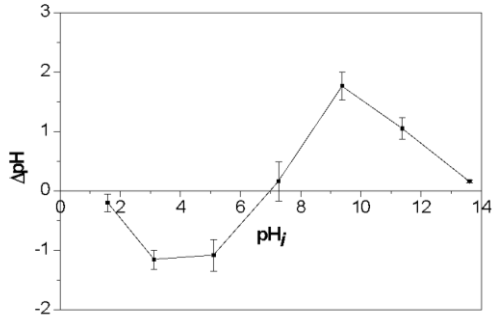


Fig. 6 Zero-charge potential (PZC) of activated carbon from cocoa biomass

The pH_{PZC} of the coal under study is similar to the range commonly reported in the literature for coals prepared from lignocellulosic residues, which generally have a pH_{PZC} between 5 and 9 depending on the precursor and activation method (Nabais et al. 2013; Saucier et al. 2015).

3.3. Adsorption studies

3.3.1. Adsorption isotherms

Adsorption isotherms are fundamental for understanding and describing the interactions between adsorbate molecules and the adsorbent's active sites. Mathematical treatments, such as the Freundlich and Langmuir models, are often used to describe the adsorption mechanism, surface characteristics, and site affinity for the adsorbate (Hameed and El-Khaiary 2008). The correlations obtained in this study for the Langmuir and the Freundlich isotherm models are presented in Figure 7.

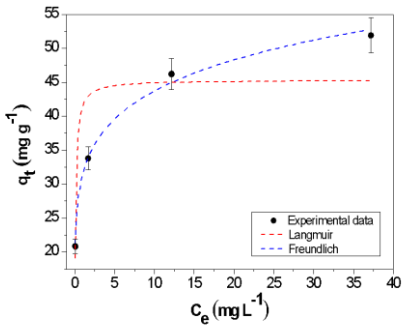


Fig. 7 Adsorption isotherm of MG on activated carbon. Correlation of adsorbed and solution MG dye in equilibrium after 4h of adsorption reaction at 30 ºC.; (Conditions: m_{ads} = 100 mg, V_{sol} = 50 mL)

As shown, after mathematical modelling, the Freundlich model best fits the results (Fig. 7, blue line). Differently from Langmuir model, which postulates that adsorption process occurs in a monolayer and all the active sites exhibit the same

energy and present a finite adsorption sites (Sartape et al. 2017), in the empirical Freundlich model, the constant *n* is directly related to the heterogeneity of the adsorbent surface and indicates the intensity of the interaction between the adsorbate and the adsorbent (Sartape et al. 2017). The higher the n value (n > 1) and the term 0 (1/n (1), the stronger the interaction, indicating a favorable process. In turn, the constant K_F represents the adsorption capacity of the material. Table 4 summarizes the parameters estimated for each isotherm model analyzed.

Table 4 Parameters obtained by the linear fit of Langmuir and Freundlich models for MG adsorption using activated carbon

Model	Parameters	Values
Langmuir	q_{max}, **cal**	45.3005
	K_L	10.6525
	R_L	0.9949
	R^2	0.6501
Freundlich	K_F	31.3234
	n	6.93526
	R^2	0.9931

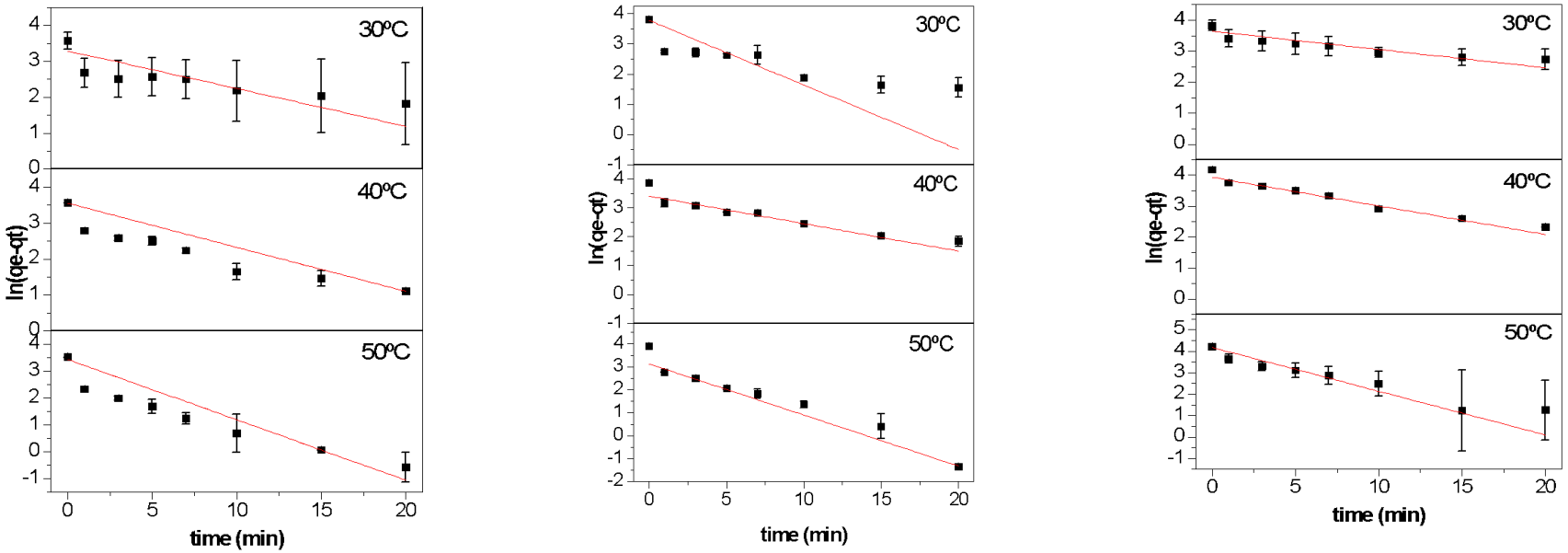
The K_F and *n* data indicate that an increase in negative charges on the adsorbent surface promotes electrostatic interactions that resemble van der Waals forces between the adsorbent surface and the dye molecules. Although factors such as dye molecular weight and size can limit adsorption, the results point to a clear predominance of adsorption capacity. The intensity of these

interactions reflects the binding energies, suggesting mild chemisorption rather than simple physisorption (Sartape et al. 2017).

3.3.2 Adsorption kinetics

Studying adsorption kinetics is essential for identifying the rate-controlling step. Understanding the kinetics also allows us to understand the adsorption mechanisms and the rate of dye adsorption. To analyze the kinetics of MG adsorption by activated carbon, the pseudo first-order, pseudo second-order, and intraparticle diffusion equations were tested at the different concentrations and temperatures studied.

Using equations 4, 5, and 6, the corresponding figures 8, 9, and 10 show the profiles for pseudo-first-order, pseudo second-order, and intraparticle diffusion behavior, respectively, in the adsorption of MG on the activated carbon. The fitting results are listed in Table 5.



(a) (b) (c)

Fig. 8 Kinetic study of adsorption *pseudo*-first order model at different temperatures for three MG concentrations: **(a)** 75 mg L^{-1}; **(b)** 100 mg L^{-1}; and **(c)** 150 mg L^{-1} (Conditions: m_{ads} =100 mg, V_{sol} =50 mL, time interval = 20 min)

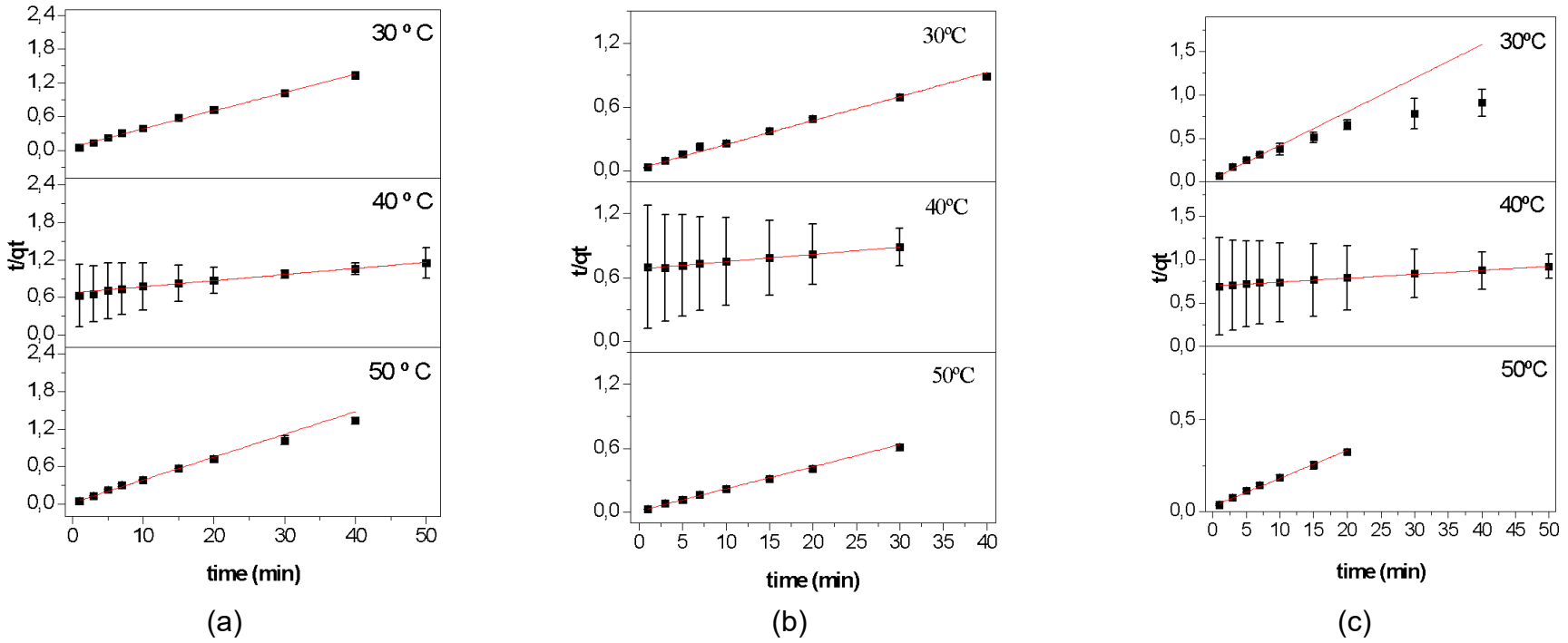


Fig. 9 Kinetic study of adsorption *pseudo*-second order model at different temperatures for three MG concentrations: **(a)** 75 mg L^{-1}; **(b)** 100 mg L^{-1}; and **(c)** 150 mg L^{-1}. (Conditions: m_{ads} =100 mg, V_{sol} =50 mL, time interval = up to 50 min)

The best fit was achieved when the PSO kinetic model was applied for any concentration of dye and any temperature tested. A recent study on MG adsorption on a composite of iron(III) nanoparticles and activated carbon showed a similar kinetic behavior during adsorption (Lincold et al. 2024). The same kinetics were observed in a report using MG (in oxalate form) in an adsorption process on argan nut shells (Sadoq et al. 2024). Also, studies on MG adsorption on KOH-activated clay aggregates showed PSO kinetic behavior (Pishdadi-Aghdarreh et al. 2025).

Once MG is a charged molecule, maybe, the adsorption can occur between the dye and the residual functional groups present in the charcoal which has been preserved from biomass. It is a reasonable hypothesis since the pH_{PZC} is almost neutral in the prepared activated carbon in this study.

Table 5 Kinetic parameters for the adsorption of MG on activated carbon, prepared from cocoa shell biomass, at different initial concentrations and temperatures

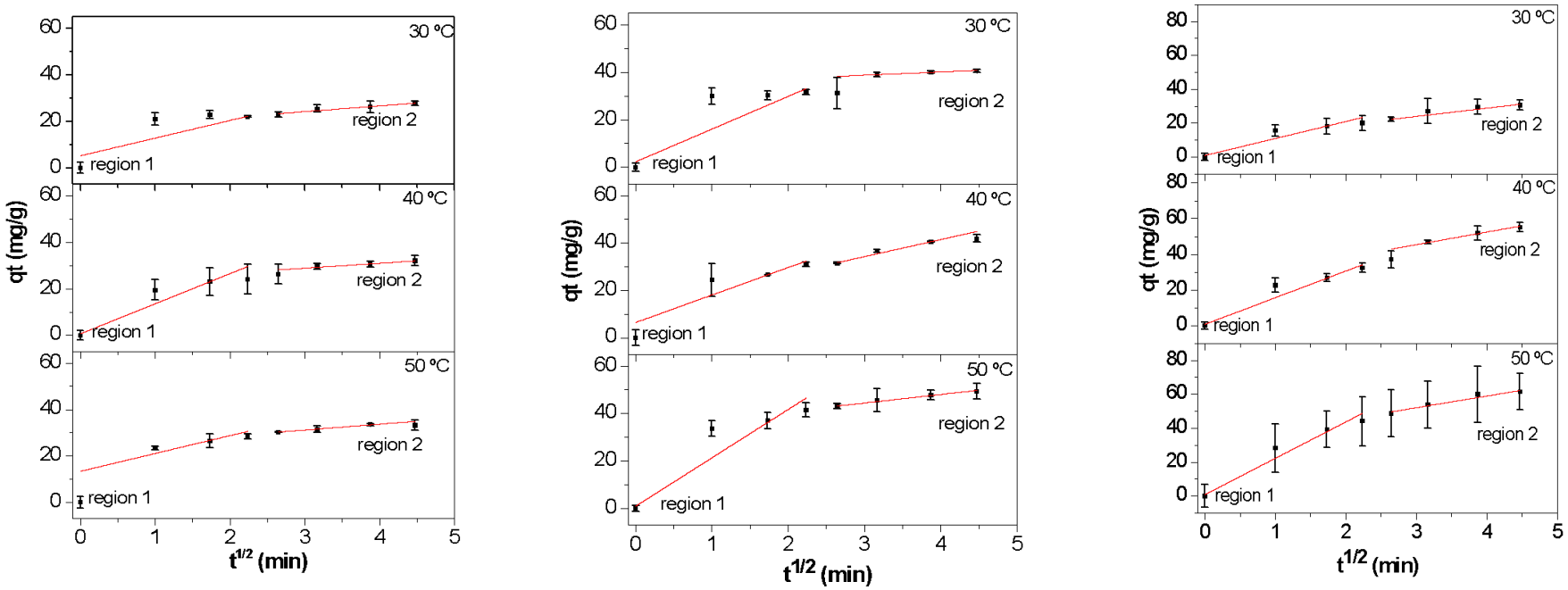
Concentration (mg L^{-1})	Temperature (ºC)	Pseudo-first order model			Pseudo second order model		
		qt (mg g^{-1})	K_1	R^2	qt (mg/g)	K_2	R^2
75	30	26.77	0.1046	0.5646	30.96	$1.87x10^{-2}$	0.9965
	40	34.76	0.1227	0.9921	103.09	$1.39x10^{-4}$	0.9860
	50	31.01	0.2242	0.9856	27.77	$6.17x10^{-2}$	0.9970
100	30	43.55	0.2136	0.6151	43.47	$2.40x10^{-2}$	0.9953
	40	30.18	0.0954	0.9314	146.19	$6.86x10^{-5}$	0.9976
	50	22.70	0.2224	0.9949	48.23	$3.76x10^{-2}$	0.9954
150	30	38.39	0.059	0.8309	25.81	$5.21x10^{-2}$	0.9643
	40	50.84	0.0922	0.8605	222.22	$2.90x10^{-2}$	0.9972
	50	30.46	0.2033	0.8775	36.36	$4.98x10^{-2}$	0.9914

Rather than the PFO and PSO kinetic models, the intraparticle diffusion model was evaluated. The adsorption curves (Fig. 10) show that the adsorption process tends to be followed by two phases (region 1 and region 2). The linearized regions indicate that the adsorption of malachite green occurred through multiple mass transfer steps. In the first stage (region 1), the adsorption of the malachite green dye occurs by diffusion in a film on the external surface of the adsorbent; in the second stage (Region 2), the diffusion of malachite green molecules occurs in the porous structures of the activated carbon, in addition to possible external adsorptions (De Andrade et al. 2021; Menezes et al. 2025).

Furthermore, the linear graphs at each concentration and temperature did not pass through the origin ($C \neq 0$), indicating that intraparticle diffusion was not the only rate-controlling step (Önal et al. 2007). The values of the intraparticle diffusion rate constant k_{int} for 75, 100, and 150 mg/L dye concentrations at 30, 40, and 50 °C are given in the Table 6.

Table 6 Kinetic data from malachite green adsorption on activated carbon modelled using intraparticle diffusion model for each dye concentration and temperature evaluated

[MG], mol/L	Temperature, ºC	Region 1			Region 2		
		ki	C	R^2	ki	C	R^2
		$mg.g^{-1}min^{-1/2}$			$mg.g^{-1}min^{-1/2}$		
	30	7.6093	5.3058	0.6315	2.4850	16.8467	0.9193
75	40	12.9630	0.6696	0.8830	2.0843	22.7020	0.7734
	50	7.6836	13.4347	0.4096	2.5110	23.6750	0.9799
	30	13.8004	2.3007	0.8727	1.3454	34.8249	0.4305
100	40	11.6006	6.5134	0.8666	7.2004	1.27119	0.9783
	50	20.4054	0.9359	0.9112	3.6092	33.6307	0.9896
	30	10.0104	1.0096	0.8754	4.8797	9.4876	0.9597
150	40	14.9245	0.8508	0.9600	7.0343	24.3928	0.8394
	50	21.4365	0.8569	0.9683	6.8957	31.4159	0.9437



(a) (b) (c)

Fig. 10 Mathematical treatment of adsorption data of MG on activated carbon from cocoa biomass according the intraparticle diffusion kinetic model. The analysis was evaluated in 2 stages (regions 1 and 2) in: **(a)** 75 mg L^{-1}; **(b)** 100 mg L^{-1}; and **(c)** 150 mg L^{-1}. (Conditions: m_{ads} =100 mg, V_{sol} =50 mL, time interval = 20 min)

3.3.3. Thermodynamic studies

Determining thermodynamic parameters is important for understanding the system's behavior in its final state. Evaluating the parameters of enthalpy, entropy, and Gibbs free energy allows us to identify whether the adsorption process is favorable, whether energy is absorbed or released, assess the spontaneity of the system, and even indicate the nature of the process (Nascimento et al. 2020).

To verify the effect of temperature on adsorption, the thermodynamic parameters enthalpy ($\Delta_{ads}H$) and entropy ($\Delta_{ads}S$) were obtained from the graph of ln Keq versus 1/T (Figure 11) and are presented in Table 7. For these estimations, the data collected at 100 mg/L of MG were used to plot the correlation between equilibrium constant vs temperature (Figure 11).

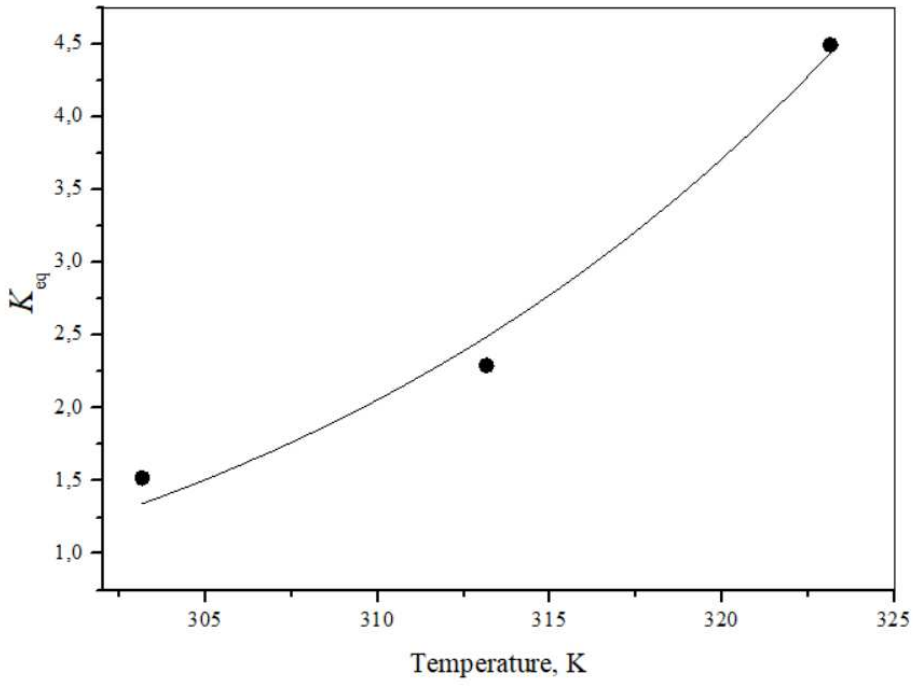


Fig. 11 Effect of temperature on MG adsorption on activated carbon derived from cocoa shell biomass

Table 7 Thermodynamic parameters for the adsorption of MG (100 mg L^{-1}) on activated carbon derived from cocoa shell biomass

T (K)	K_{eq}	$\Delta H°_{ads}$ (kJ mol^{-1})	$\Delta S°_{ads}$ (J mol^{-1} K^{-1})	$\Delta G°_{ads}$ (kJ mol^{-1})
303.15	1.52 ± 0.07			-0.745
313.15	2.29 ± 0.12	48.65	162.9	-2.374
323.15	4.49 ± 1.62			-4.003

The positive ΔH_{ads} value confirms the endothermic nature of the adsorption, and the high calculated values indicate that it is not physisorption. Enthalpy values above 40 kJ.mol^{-1} suggest that adsorption is driven by chemisorption mechanism, as reported and concluded in a study on methylene blue adsorption on palm date seed (Sadi et al. 2025). On the other hand, physisorption results in very small enthalpy values, as reported in the study of phenol adsorption on granular activated carbon (Sadi et al. 2025).

The positive ΔS_{ads} value indicates the assembly between dye molecules and the adsorbate surface. The positive value indicates a favorable interaction. Finally, the higher is the temperature, more spontaneous the adsorptions can occur, since the Gibbs energy is becoming more negative, as can be seen in Table 7. The mathematical treatment for 150 mg L^{-1} of dye at 303.15 K resulted in a positive Gibbs energy (not shown). A similar behavior was described in studies of oxytetracycline removal from aqueous solution using activated carbon from barley lignocellulosic wastes (Kazemi et al. 2024). Such scenario can indicate a complex mechanism.

Correlating the thermodynamic parameters with the kinetic data suggests that the adsorption phenomenon in the studied scenario is complex and can

ultimately follow a different pathway depending on the reaction temperature. The mechanism, eventually, can consider not only the interaction between the dye and the solid phase surface, but also the effect of intra-particule diffusion, as explained before (Table 6 and Fig. 10).

The infrared spectra of biomass (a), malachite green (b), activated carbon (c), activated carbon after contact with the dye solution (d) are shown in Figure 12.

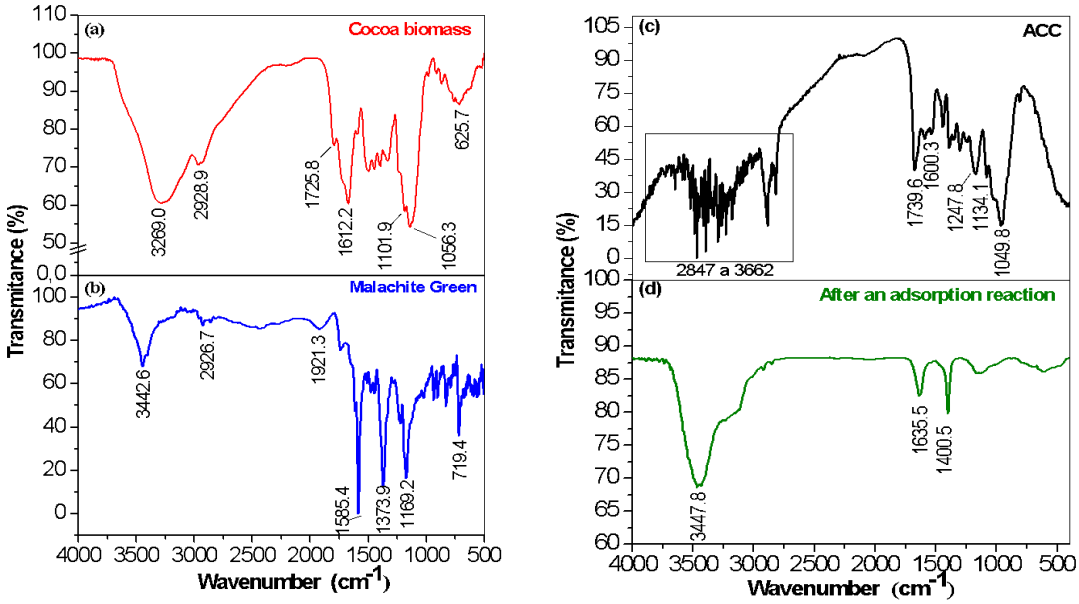


Fig. 12 Infrared spectrum of **(a)** cocoa biomass, **(b)** malachite green **(c)** carbon and **(d)** carbon after adsorption of MG

The infrared spectrum of cocoa biomass is presented in Figure 12.a. The band around 3269 cm^{-1} is attributed to angular deformation stretching of OH groups in water or the structure of biomass macrocomponents (hemicellulose, cellulose, and lignin). The bands between 2928 cm^{-1} indicate asymmetric and symmetric stretching of C-H groups present in the aliphatic or aromatic chain. Bands at 1612 cm^{-1} are mainly due to the presence of C=C bonds and

symmetrical bending vibrations of -CH_3. The band at 1056 cm^{-1} corresponds to C=O stretching vibrations, and the signals presented in the ranges 1700-1730 cm^{-1} and 1510-1560 cm^{-1} represent the carbonyl functional group present in the structure of biomass components, such as the carboxylic acid group present in hemicellulose. A band at approximately 625 cm^{-1} is characteristic of the deformation of aromatic hydrocarbons (Fiuza-Junior et al. 2016).

The bands highlighted in the infrared spectrum of the MG dye, Figure 12.b, under study are, 3443 cm^{-1} corresponding to the NH_2 stretching; at 1585 cm^{-1} corresponding to the C=C stretching vibration of the benzene ring; at 1169 cm^{-1} and 1374 cm^{-1} corresponding to C ─ N stretching vibrations; At 719 cm^{-1} it is characteristic of the presence of aromatic groups. The bands at approximately 1170 cm^{-1} correspond to the C ─ N stretching vibrations, and at approximately 2926 cm^{-1} correspond to the C ─ H stretching of the asymmetric CH_3 group. The bands observed in the spectrum of the dye under study are in good agreement with those reported by Cheriaa et al. (2012) and Pourbabae et al. (2013).

Figure 12.c and 12.d show the vibrational spectra before and after an adsorption experiment of MG dye, respectively. For activated carbon before the adsorption, bands are observed at ~1049 cm^{-1}, 1247 cm^{-1}, 1739 cm^{-1}, and in the range from 2847 cm^{-1} to 3662 cm^{-1}. The bands presented at approximately 1600 cm^{-1} can be attributed to the stretching of the C=C bond constituting the aromatic benzene molecules. The bands near 1100 cm^{-1} are attributed to C-O stretching vibrations of phenolic groups. These characteristics were also observed in studies by De Sales and collaborators on activated carbons derived from agro-industrial waste (De Sales et al. 2015).

Analyzing the vibration spectrum of activated carbon after adsorption of MG (Figure 12.d), it is observed that some bands that appeared in the carbon spectrum in the region from 2847 cm^{-1} to 3662 cm^{-1} do not appear, in this region, only one band is observed at ~3447 cm^{-1}, evidencing the presence of dye adsorbed on the activated carbon surface. Comparing the activated carbon vibrational spectra before and after MG adsorption, it can be seen that bands could indicate a bond between the dye and the adsorbent surface, since such bands were not seen in MG or in activated carbon separately. By such analysis, it is evident that the chemisorption is the phenomenon that can take place in the scenario of the study carried out herein.

4. Conclusion

It has been demonstrated that cocoa husk biomass can be used as a sustainable raw material for the production of activated carbons following the preparation method used in this work. Using low-value residual biomass to produce value-added materials makes the final product cheaper and has a positive environmental impact by avoiding improper disposal. The material obtained was fully characterized and exhibited important properties that enable its use in filtration/adsorption systems. The kinetic data showed behavior consistent with the PSO model, and the adsorption isotherm fit the Freundlich model better. Those results allowed us to conclude that chemisorption is the driving force for the process. Thermodynamic data, including a high enthalpy and a temperature-dependent Gibbs free energy, corroborated this observation.

Acknowledgements

We are grateful for the fellowships of Institutional Program for Technological Development and Innovation Initiation Scholarships (PIBITI) offered by the National Council for Scientific and Technological Development (CNPq) and the Federal University of Recôncavo da Bahia (2022-2023) attributed to L.O. Galvão.

Statements and Declarations

Author Contribution

Lourdes Oliveira Galvão: Experimental Data, Conceptualization, Methodology, Investigation, Data Curation and Formal Analysis and Writing–original draft. Gabriel Santos dos Anjos: Experimental Data, Data Curation, Investigation and Writing–editing. Artur José Santos Mascarenhas: Supervision, Resources, Formal Analysis and Writing–review. Raildo Alves Fiuza-Junior: Supervision, Resources, Formal Analysis and Writing–review. Gerônimo Lopes Lima: Conceptualization. Rodrigo De Paula: Conceptualization, Methodology, Formal Analysis and Writing–review and editing.

Funding

The article processing charge for the publication of this work was funded by the Coordination for the Improvement of Higher Education Personnel (CAPES). The research was funded by the National Council for Scientific and Technological Development (CNPq) through the Institutional Program for Technological Development and Innovation Initiation Scholarships (PIBITI) nº 22184/2021-1; 2021-2022 and and the Federal University of Recôncavo da Bahia during 2022-2023.

Data Availability

The authors confirm that all data supporting this research are available within the article.

Ethical approval This is not applicable. This study does not contain any studies with human participants or animals performed by any of the authors.

Consent to participate This is not applicable. This study does not contain any studies with human participants or animals performed by any of the authors.

Consent for publication This is not applicable. This study does not contain any studies with human participants or animals performed by any of the authors.

Competing interests The authors have no relevant financial or non-financial interests to disclose

References

Abewaa M, Mengistu A, Takele T, Fito J, Nkambuke T (2023) Adsorptive removal of malachite green dye from aqueous solution using Rumex abyssinicus derived activated carbon. Sci Rep 13:14701. https://doi.org/10.1038/s41598-023-41957-x

Ahmad AA, Ahmad MA, Yahaya NKEM, Karim J (2021) Adsorption of malachite green by activated carbon derived from gasified Hevea brasiliensis root. Arab J Chem 14:103104. https://doi.org/10.1016/j.arabjc.2021.103104

Al-Asadi ST, Mussa ZH, Al-Qaim FF, Kamyab H, Al-Saedi HFS, Deyab IF, Kadhim NJ (2025) A comprehensive review of methylene blue dye adsorption on activated carbon from edible fruit seeds: A case study on kinetics and adsorption models. Carbon Trends 20:100507. https://doi.org/10.1016/j.cartre.2025.100507

Alfa KA, Meza-Sepulveda DC, Vaulot C, Le Meins J-M, Ghimbeu CM, Tonini L, Cubillos JA, Moynault L, Platel V, Paredes D, Hort C (2024) Cocoa Pod Husk Carbon Family for Biogas Upgrading: Preliminary Assessment Using the Approximate Adsorption Performance Indicator. *C* 2024, 10:100. https://doi.org/10.3390/c10040100

Anoraga SB, Shamsudin R, Hamzah MH, Sharif S, Saputro AD (2024) Cocoa by-products: A comprehensive review on potential uses, waste management, and emerging green technologies for cocoa pod husk utilization. Heliyon 10:e35537. https://doi.org/10.1016/j.heliyon.2024.e35537

Cai J, Qi J, Yang C, Zhao X (2014) Poly(vinylidene chloride)-Based Carbon with Ultrahigh Microporosity and Outstanding Performance for CH4 and H2 Storage and CO2 Capture. ACS Appl. Mater. Interfaces 6:3703–3711. https://doi.org/10.1021/am500037b

Cheriaa J, Khaireddine M, Rouabhia M, Bakhrouf A (2012) Removal of Triphenylmethane Dyes by Bacterial Consortium. The Scientific World Journal 2012:512454. https://doi.org/10.1100/2012/512454

Da Silva JPS, Barral AVS, Azevedo LEC, Oliveira TS, de Sousa AAO, Nobre JRC, Sousa VC (2021) Activated carbon from cashew nut fruit mesocarp (Anacardium occidentale) in the removal of dye in aqueous medium [Carvão ativado oriundo do mesocarpo do fruto da castanha de caju (Anacardium occidentale) na remoção de corante em meio aquoso]. Res Soc Dev 10:21710313221. https://doi.org/10.33448/rsd-v10i3.13221 (in Portuguese)

Dantas SC, Teixeira GF, Ferrari JG, Ruy LM, Trindade RS, Carmello V de O (2020) Adsorption of malachite green dye using banana peel and corn cob as adsorbent [Adsorção do corante verde de malaquita utilizando casca de banana e sabugo de milho como adsorvente]. Rev Bras Cienc Tecnol Inov 5:124–139. https://doi.org/10.18554/rbcti.v5i2.3839 (in Portuguese)

De Andrade RC, Menezes RSG, Fiuza-Jr RA, Andrade HMC (2021) Activated carbon microspheres derived from hydrothermally treated mango seed shells for acetone vapor removal. Carbon Lett 31:779-793 https://doi.org/10.1007/s42823-020-00184-4

De Sales PF, Bertoli AC, Pinto FM, Magriotis ZM (2015) Production, Characterization and Application of Activated Carbon Obtained from the Corncob: The Search for the Reuse of an Agroindustrial Waste. Rev Virtual Quim, 7:1174–1188. https://doi.org/10.5935/1984-6835.20150066

De Sousa AAO, Oliveira TS, de Azevedo LEC, Nobre JRC, Stefanelli WFR, de Sousa Costa TAP, Barral AVS (2021) Adsorption of the basic Malachite Green dye via activated carbon from the açaí seed. Res Soc Dev 10:e49110212871. https://doi.org/10.33448/rsd-v10i2.12871

El Meziani S, Agnaou H, El Haddaj H, Boumya W, Barka N, Elhalil A (2025) Sustainable adsorption technologies for textile dye removal: advances in biomass-derived and magnetically modified activated carbons. Cleaner Chem Eng 12:100210. https://doi.org/10.1016/j.clce.2025.100210

Enayatpour B, Rajabi M, Moradi O, Asdolehzade N, Nayak A, Agarwal S, Gupta VK (2018) Adsorption kinetics of lysozyme on multi-walled carbon nanotubes and

amino functionalized multi-walled carbon nanotubes from aqueous solution. J Mol Liq 254:93-97. https://doi.org/10.1016/j.molliq.2018.01.079

Essandoh M, Wolgemuth D, Pittman CU, Mohan D, Mlsna T (2016) Adsorption of metribuzin from aqueous solution using magnetic and nonmagnetic sustainable low-cost biochar adsorbents. Environ Sci Pollut Res, 24:4577–4590. https://doi.org/10.1007/s11356-016-8188-6

Ferrão-Gonzales AD, Vital AVD, Lima JM, Rodrigues MBS (2013) Development of a sustainable cocoa culture based on its waste recovery. Interfaces Cient Saude Ambiente 1(2):41–52. https://doi.org/10.17564/2316-3798.2013v1n2p41-52

Fiuza-Junior RA (2016) Valorization of regional fruit stones and CO2 capture [Valorização de caroços de frutas regionais e captura de CO2]. PhD Thesis, Federal University of Bahia, Salvador (in Portuguese) http://repositorio.ufba.br/ri/handle/ri/26187

Fiuza-Junior RA, Andrade RC, Andrade HMC (2016) CO_2 capture on KOH-activated carbons derived from yellow mombin fruit stones. J Environ Chem Eng 4:4229–4236. https://doi.org/10.1016/j.jece.2016.09.025

Girón-Hernández J, Tombe A, Koyilot MC, Salas-Calderón KT, Charlton A, Wills C, Gentile P (2024) From cocoa waste to sustainable bioink: valorising pectin for circular economy-driven tissue engineering. Eur Polym J, 210:112967. https://doi.org/10.1016/j.eurpolymj.2024.112967

Hameed BH, El-Khaiary MI (2008) Equilibrium, Kinetics and Mechanism of Malachite Green Adsorption on Activated Carbon Prepared from Bamboo by

K2CO3 Activation and Subsequent Gasification with CO2. J Hazard Mater , 157:344–351. https://doi.org/10.1016/j.jhazmat.2007.12.105

IBGE (2025) Cocoa production [Produção de Cacau]. Brazilian Institute of Geography and Statistics (IBGE). https://www.ibge.gov.br/explica/producao-agropecuaria/cacau/pa. Accessed 13 Feb 2026 (in Portuguese)

Kazemi A, Ebrahimpour E, Esmaeilbeigi M, Gheitasi F, Einollahipeer F, Mohammadrezai M (2024) Optimizing oxytetracycline removal from aqueous solutions using activated carbon from barley lignocellulosic wastes with isotherms and thermodynamic studies. Sci Rep, 14:23281. https://doi.org/10.1038/s41598-024-73142-z

Largitte L, Pasquier R (2016) Chem Eng Res Des a review of the kinetics adsorption models and their application to the adsorption of lead by an activated carbon. Chem Eng Res Des 109:495–504. https://doi.org/10.1016/j.cherd.2016.02.006

Lincold MN, Jules ML, Guy NP, Suzanne M, Jacques MB, Sylvain T, Shikuku VO, Tchieta GP (2024) Enhanced adsorption of malachite green onto a composite material activated carbon and iron (III) oxide nanoparticles: isotherm, kinetic, and thermodynamic study. Biomass Convers Biorefin 15:28497-28516. https://doi.org/10.1007/s13399-024-06277-8

Menezes RSG, Cordeiro JLC, de Andrade RC (2025) VOC removal on activated biochar prepared from the invasive aquatic plant *Eichhornia crassipes* for air decontamination by temperature swing adsorption process. Environ Sci Pollut Res 32:20509–20527. https://doi.org/10.1007/s11356-025-36854-x

Nabais JMV, Laginhas C, Carrott MMLR, Carrott PJM, Crespo-Amorós JE, Nadal-Gisbert AV (2013) Surface and porous characterisation of activated carbons made from a novel biomass precursor, the esparto grass. Appl Surf Sci 265:919–924. https://doi.org/10.1016/j.apsusc.2012.11.164

Nascimento RF, Vidal CB, Raulino GS, Melo D (2020) Adsorption: Theoretical aspects and environmental applications [Adsorção: Aspectos teóricos e aplicações ambientais]. Imprensa Universitária, Fortaleza (in Portuguese)

Neme I, Gonfa G, Masi C (2022) Activated carbon from biomass precursors using phosphoric acid: A review. Heliyon 8:e11940. https://doi.org/10.1016/j.heliyon.2022.e11940

Oliveira MHGD (2024a) Preparation and characterization of adsorbent derived from carnauba waste (Copernicia prunifera) for malachite green dye adsorption [Obtenção e caracterização de adsorvente proveniente de resíduos da carnaúba (Copernicia prunifera) para adsorção do corante verde de malaquita]. MSc Dissertation, Federal Rural University of the Semi-Arid, Mossoró (in Portuguese) https://repositorio.ufersa.edu.br/bitstreams/14006be6-02e7-4138-a387-d013d847cc87/download

Oliveira MNMFD (2024b) Adsorption kinetics of malachite green dye on silk flower fibers (Calotropis procera) [Cinética de adsorção do corante verde malaquita em fibras de flor-de-seda (Calotropis Procera)]. MSc Dissertation, Federal Rural University of the Semi-Arid, Mossoró (in Portuguese) https://repositorio.ufersa.edu.br/items/d8b2f13a-1706-466e-b773-efdfd1b26136/full

Olofsson J, Börjesson P (2018) Residual biomass as resource–Life-cycle environmental impact of wastes in circular resource systems. *J Clean Prod*, 196:997-1006. https://doi.org/10.1016/j.jclepro.2018.06.115

Önal Y, Akmil-Başar C, Sarıcı-Özdemir Ç (2007) Investigation Kinetics Mechanisms of Adsorption Malachite Green onto Activated Carbon. J Hazard Mater 146:194–203. https://doi.org/10.1016/j.jhazmat.2006.12.006

Pereira RG, Veloso CM, da Silva NM, de Sousa LF, Bonomo RCF, de Souza AO, Fontan RDCI (2014) Preparation of activated carbons from cocoa shells and siriguela seeds using H_3PO_4 and $ZnCl_2$ as activating agents for BSA and α-lactalbumin adsorption. Fuel Process Technol 126**:**476–486. https://doi.org/10.1016/j.fuproc.2014.06.001

Pishdadi-Aghdarreh F, Norouzbeigi R, Velayi E (2025) KOH-activated lightweight expanded clay aggregate (LECA) for malachite green adsorption: activation mechanism and adsorption process assessment. Int J Environ Sci Technol 22:5633–5654. https://doi.org/10.1007/s13762-024-06212-4

Pourbabaee AA, Ramezani S, Javaheri Daneshmand H (2013) Biodegradation of malachite green by Klebsiella Terrigenaptcc 1650: the critical parameters were optimized using Taguchi optimization method. J Bioremed Biodegrad 4:175. https://doi.org/10.4172/2155-6199.1000175

Raval NP, Shah PU, Shah NK (2016) Malachite green “a cationic dye” and its removal from aqueous solution by adsorption. Appl Water Sci 7:3407–3445. https://doi.org/10.1007/s13201-016-0512-2

Rout T, Pradhan D, Singh RK, Kumari N (2016) Exhaustive study of products obtained from coconut shell pyrolysis. J Environ Chem Eng 4:3696–3705. https://doi.org/10.1016/j.jece.2016.02.024

Sá IMGL (2021) Synthesis of Fe3O4/MgAl-LDH magnetic composite and its precursor materials for adsorptive removal of malachite green in aqueous medium [Síntese do compósito magnético Fe3O4/HDL-MgAl e seus materiais precursores para remoção adsortiva de verde malaquita em meio aquoso]. MSc Dissertation, Federal University of Alagoas, Maceió (in Portuguese) https://www.repositorio.ufal.br/handle/123456789/8453

Sadi M, Namane A, Azri YM, Tou I (2025) Adsorption and Desorption of Phenol onto Granular Activated Carbon: Kinetics and Thermodynamic Studies. J Solution Chem 54:906–932. https://doi.org/10.1007/s10953-025-01458-z

Sadoq M, Imame S, Atlas H, Ouchabi M, Kali A, Sadoq B-E, Amar A, Loulidi I, Jabri M, Alrashdi AA, Lgaz H, Bennani MN, Boukhlifi F (2024) Utilization of argan nut shells as a bioresource for efficient malachite green oxalate adsorption. Chem Pap 78:7525–7540. https://doi.org/10.1007/s11696-024-03611-2

Santos CP (2020) Adsorption of leuco malachite green on biochar synthesized from pineapple crowns [Adsorção de leuco verde malaquita em biocarvão sintetizado a partir de coroas de abacaxi]. MSc Dissertation, Federal University of Espírito Santo, Vitória (in Portuguese) https://repositorio.ufes.br/items/f7cebdcb-5a51-454a-84cf-f8327402f0d0

Sartape AS, Mandhare AM, Jadhav VV, Raut PD, Anuse MA, Kolekar SS (2017) Removal of malachite green dye from aqueous solution with adsorption technique

using Limonia acidissima (wood apple) shell as low cost adsorbent. Arab J Chem 10:S3229–S3238. https://doi.org/10.1016/j.arabjc.2013.12.019

Saucier C, Adebayo MA, LIMA EC, Cataluña R, Thue PS, Prola LDT, Puchana-Rosero MJ, Machado FM, Pavan FA, Dotto GL (2015) Microwave-assisted activated carbon from cocoa shell as adsorbent for removal of sodium diclofenac and nimesulide from aqueous effluents. J Hazard Mater 289:18–27. https://doi.org/10.1016/j.jhazmat.2015.02.026

Sherwood J (2020) The significance of biomass in a circular economy. Bioresour Technol 300:122755. https://doi.org/10.1016/j.biortech.2020.122755

Silva AAD (2021) Evaluation of in natura green coconut fiber (Cocos nucifera Linn.) as an alternative adsorbent for synthetic malachite green dye removal [Avaliação da fibra de côco verde in natura (Coco nucífera Linn.) como um adsorvente alternativo para remoção do corante sintético verde malaquita]. MSc Dissertation, Federal University of Alagoas, Maceió (in Portuguese) https://www.repositorio.ufal.br/handle/123456789/8135

Silva LF (2014) Use of sawdust powder as an alternative adsorbent in malachite green removal [Utilização do pó de serragem como adsorvente alternativo na remoção de verde de malaquita]. MSc Dissertation, Federal University of Technology – Paraná, Curitiba (in Portuguese) https://repositoriocopia.utfpr.edu.br/jspui/handle/1/6271

Sotelo-Coronado LE, Oviedo-Argumedo W, Alvis-Bermúdez A (2025) Cacao in the Circular Economy: A Review on Innovations from Its By-Products. *Processes* 13:2098. https://doi.org/10.3390/pr13072098

Suresh S, Chandra Srivastava V, Mani Mishra I (2011) Adsorption of Hydroquinone in Aqueous Solution by Granulated Activated Carbon. J Environ Eng 137:1145–1157. https://doi.org/10.1061/(asce)ee.1943-7870.0000443

Swan NB, Zaini MAA (2019) Adsorption of Malachite Green and Congo Red Dyes from Water: Recent Progress and Future Outlook. Ecol Chem Eng S 26:119–132. https://doi.org/10.1515/eces-2019-0009

Xu A, Wu YH, Chen Z, Wu G, Wu Q, Ling F, Huang WE, Hu HY (2020) Towards the new era of wastewater treatment of China: development history, current status, and future directions. Water Cycle 1:80–87. https://doi.org/10.1016/j.watcyc.2020.06.004

Zaharia C, Musteret C-P, Afrasinei M-A (2024) The Use of Coagulation–Flocculation for Industrial Colored Wastewater Treatment—(I) The Application of Hybrid Materials. Appl Sci 14:2184. https://doi.org/10.3390/app14052184

Zanoni MVB, Yamanaka H (2016) Dyes: Chemical and toxicological characterization, detection methods, and treatment [Corantes: Caracterização química, toxicológica, métodos de detecção e tratamento]. Cultura Acadêmica, São Paulo (in Portuguese)

Zhang S, Gao H, Huang Y, Wang X, Hayat T, Li J, Xu X, Wang X (2018) Ultrathin g-C3N4 nanosheets coupled with amorphous Cu-doped FeOOH nanoclusters as 2D/0D heterogeneous catalysts for water remediation. Environ Sci Nano 5:1179–1190. https://doi.org/10.1039/c8en00124c